

A TEXTBOOK EXAMPLE OF A BOW SHOCK IN THE MERGING GALAXY CLUSTER 1E0657-56

M. MARKEVITCH, A. H. GONZALEZ, L. DAVID, A. VIKHLININ, S. MURRAY, W. FORMAN, C. JONES,
W. TUCKER¹

Harvard-Smithsonian Center for Astrophysics, 60 Garden St., Cambridge, MA 02138; maxim@head-cfa.harvard.edu

ApJ Letters in press; astro-ph/0110468 v2

ABSTRACT

The *Chandra* image of the merging, hot galaxy cluster 1E0657-56 reveals a bow shock propagating in front of a bullet-like gas cloud just exiting the disrupted cluster core. This is the first clear example of a shock front in a cluster. From the jumps in the gas density and temperature at the shock, the Mach number of the bullet-like cloud is 2–3. This corresponds to a velocity of 3000–4000 km s⁻¹ relative to the main cluster, which means that the cloud traversed the core just 0.1–0.2 Gyr ago. The 6–7 keV “bullet” appears to be a remnant of a dense cooling flow region once located at the center of a merging subcluster whose outer gas has been stripped by ram pressure. The bullet’s shape indicates that it is near the final stage of being destroyed by ram pressure and gas dynamic instabilities, as the subcluster galaxies move well ahead of the cool gas. The unique simplicity of the shock front and bullet geometry in 1E0657-56 may allow a number of interesting future measurements. The cluster’s average temperature is 14–15 keV but shows large spatial variations. The hottest gas ($T > 20$ keV) lies in the region of the radio halo enhancement and extensive merging activity involving subclusters other than the bullet.

Subject headings: Galaxies: clusters: individual (1E0657-56) — intergalactic medium — X-rays: galaxies

1. INTRODUCTION

Galaxy clusters form via mergers of smaller subunits. Such mergers dissipate a large fraction of the subclusters’ vast kinetic energy through gas dynamic shocks, heating the intracluster gas and probably accelerating high energy particles (e.g., Sarazin 2001 and references therein). Shocks contain information on the velocity and geometry of the merger. They also provide a unique laboratory for studying the intracluster plasma, including such processes as thermal conduction and electron-ion equilibration (e.g., Shafranov 1957; Takizawa 1999). Some exploratory uses of X-ray data on cluster shocks were described by Markevitch, Sarazin, & Vikhlinin (1999). While many merging clusters exhibit recently heated gas (e.g., Henry & Briel 1995; Markevitch et al. 1999, Furusho et al. 2001 and references in those works; Neumann et al. 2001), so far only two candidate merger shock fronts were observed. One is a mild X-ray brightness edge, apparently a shock with a Mach number near 1, preceding the prominent “cold front” in A3667 (Vikhlinin, Markevitch & Murray 2001). Another is a hot region in front of the A665 core (Markevitch & Vikhlinin 2001, hereafter MV) which shows no clear density jump perhaps because of an unfavorable viewing geometry.

The *Chandra* observation of 1E0657-56 presents the first clear example of a cluster bow shock. This $z = 0.296$ cluster was discovered by Tucker, Tananbaum, & Remillard (1995) as an *Einstein* IPC extended source. From *ASCA* data, Tucker et al. (1998, hereafter T98) derived a temperature around 17 keV, making this system one of the hottest known (see also Yaqoob 1999; Liang et al. 2000, hereafter LHBA). *ROSAT* data showed that 1E0657-56 is a merger (T98). It also hosts the most luminous synchrotron radio halo (LHBA).

Below we present results from the *Chandra* observation of 1E0657-56 performed in October 2000. We use $H_0 = 100h$ km s⁻¹ Mpc⁻¹ and $\Omega_0 = 0.3$, $\Lambda = 0$; $1' = 0.172h^{-1}$ Mpc at the cluster redshift. Confidence intervals are 90% for one-

parameter, unless specified otherwise.

2. DATA ANALYSIS

1E0657-56 was observed by ACIS-I at the focal plane temperature of -120°C for a useful exposure of 24.3 ks. To derive the gas temperature for a given region of the cluster image, the telescope and detector response were modeled as described in MV. The ACIS background rate did not vary during the exposure, but was higher than expected by a factor of about 1.3, most likely due to anomalous “space weather”. This required special background modeling. To do this, we extracted a spectrum from the ACIS-I region outside an $r = 8.6'$ ($1.5h^{-1}$ Mpc) circle centered on the cluster, which should be free of cluster emission. Point sources were excluded. The observed excess over the nominal background² was well-modeled in the 0.7–10 keV band by the sum of two power laws E^{α} with photon indices $\alpha = -0.6$ and $+3.0$ (dominant below and above $E \sim 5$ keV, respectively) originating inside the detector, i.e., without applying mirror effective area and CCD efficiency to the model. Such a background anomaly in the ACIS-I chips is rare and not yet understood. We assumed that this component is distributed uniformly over the detector, and added it (normalized by solid angle) to the nominal background spectra. High-energy residuals in the overall cluster fit indicated that the normalization of the corrected background required an additional 10% increase (perhaps indicating some spatial nonuniformity of the excess), which we applied to the spectra from all cluster regions.

To make a 0.5–5 keV image for the gas density analysis, we compared the observed background rate far from the cluster to the nominal model background (without the above additional component) and derived a correction factor of 1.35 for this wide band, which was applied to the model background image. This is of course consistent with the above spectral correction. A 10% background uncertainty was included in deriving the confidence intervals for all quantities. This approxi-

¹Also at UCSD.

²A combination of blank field observations normalized by the exposure time, see <http://asc.harvard.edu/cal>, click “ACIS”, then “ACIS Background”

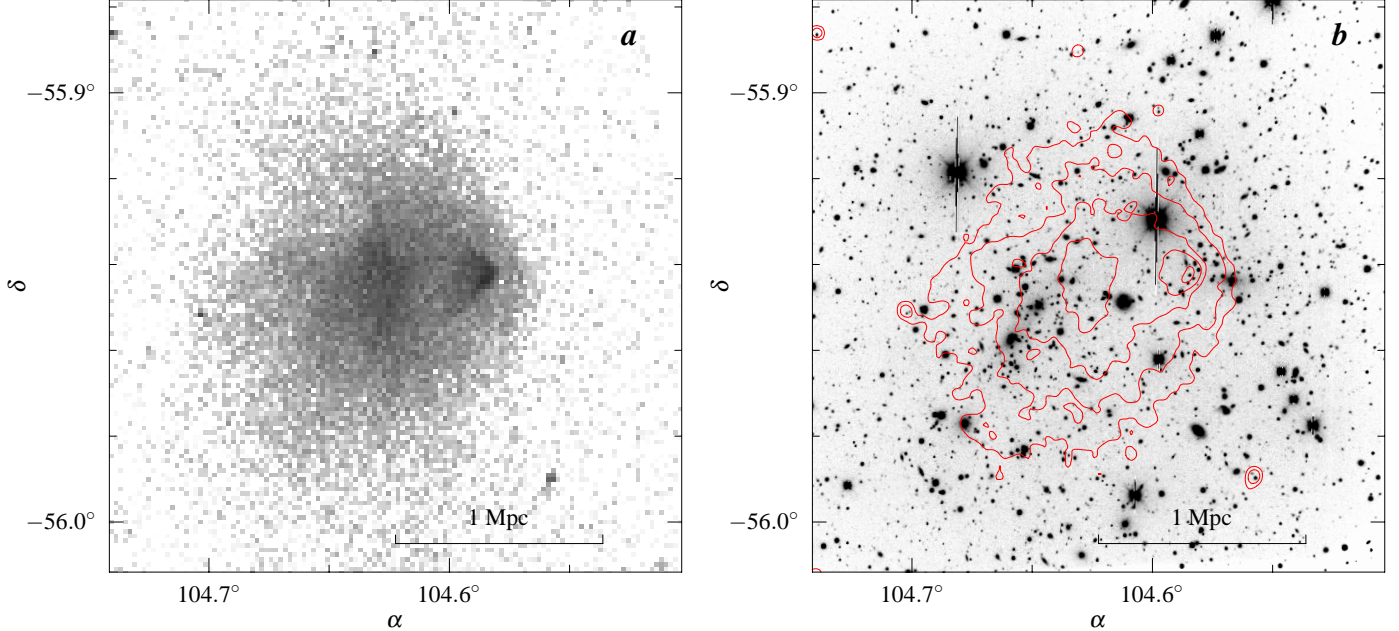


FIG. 1.—(a) ACIS 0.5–5 keV image. Pixels are $4''$; linear scale is for $h = 0.5$. (b) Grayscale shows optical R -band image from ESO NTT (courtesy of E. Falco and M. Ramella). Contours, spaced by a factor of 2, show the smoothed ACIS image. The western part of the outer contour is approximately at the shock position. A number of well-matched point sources shows that the coordinates are accurate.

mate background modeling is adequate for our present qualitative study.

To minimize the effects of calibration uncertainties, the spectra were extracted in the 0.9–9.5 keV energy band, excluding the 1.8–2.2 keV interval around the mirror Ir edge.

3. RESULTS

The ACIS image of the cluster is shown in Fig. 1a. It shows a “bullet” apparently just exiting the cluster core and moving westward. This subcluster was previously seen in the *ROSAT* data (e.g., T98), but the high resolution *Chandra* image makes its nature and direction of motion clear. The bullet is preceded by an X-ray brightness edge that resembles a bow shock. To determine whether it is indeed a shock (and not a “cold front”, e.g., Markevitch et al. 2000; Vikhlinin et al. 2001), below we derive the gas temperatures on both sides of the feature (see §3.1). Figure 1b shows X-ray contours overlaid on an optical image. A subcluster of galaxies (e.g., Barrena et al. 2001) is seen leading the X-ray bullet, which is apparently swept back from the galaxies by the ram pressure of the ambient cluster gas.

3.1. Temperature Map

We first fit an overall cluster spectrum within $r = 3'$ ($0.5 h^{-1}$ Mpc) as described in §2 using the Kaastra (1992) plasma model. We obtain $T = 14.8^{+1.7}_{-1.2}$ keV and an abundance of 0.11 ± 0.11 solar, fixing the absorption at $N_H = 4.6 \times 10^{20} \text{ cm}^{-2}$ as derived by LHBA from radio and *ROSAT* PSPC data. This temperature agrees with their *ASCA* + *ROSAT* fit of $14.5^{+2.0}_{-1.7}$ keV and is consistent with the 17.4 ± 2.5 keV *ASCA* fit by T98. If $N_H = 6.5 \times 10^{20} \text{ cm}^{-2}$ from Dickey & Lockman (1990) is used instead, we obtain $T = 13.6$ keV. When N_H is fit as a free parameter, it is consistent with both those values; the present low-energy ACIS-I calibration is not reliable for measuring N_H independently. Below we fix $N_H = 4.6 \times 10^{20} \text{ cm}^{-2}$. Within the $r = 0.5 h^{-1}$ Mpc aperture, the cluster’s 0.5–5 keV

(rest-frame) luminosity is $8.7 \pm 0.5 \times 10^{44} h^{-2} \text{ erg s}^{-1}$ and $L_{\text{bol}} = 2.3 \pm 0.2 \times 10^{45} h^{-2} \text{ erg s}^{-1}$.

Figure 2 shows a temperature map made by dividing the cluster image into several regions and fitting their temperatures and abundances as above. Despite large uncertainties, the map shows that the gas outside the shock feature (region P) is cooler, or at least not hotter, than that inside (region S), confirming that it is indeed a shock front. The temperature at the tip of the bullet is low (~ 7 keV) and is likely to have been the temperature of the subcluster. The hottest region of the cluster is its southeastern X-ray brightness elongation. The optical image shows several large galaxies in that area, suggesting that this is the main merger site. As seen in Fig. 3, this also is where the radio halo is enhanced (LHBA). The halo also extends to the western shock front. A spatial correlation between the halo brightness and the local gas temperature (in addition to the general similarity to the X-ray brightness, e.g., LHBA; Govoni et al. 2001) was noticed by MV in two other merging clusters and supports the merger shock origin for the relativistic halo electrons (e.g., Tribble 1993).

4. DISCUSSION

4.1. The shock front

The temperature map confirms that the western X-ray brightness edge is a shock front. We can derive its Mach number from either the temperature or density jump across the front using the Rankine-Hugoniot shock adiabat. Figure 4a shows an X-ray brightness profile in a 120° sector centered on the bullet’s center of curvature and directed along its apparent motion. There are two brightness edges whose shapes indicate spherical gas density discontinuities in projection. We fit this profile by the projection of a gas density model consisting of two power laws r^α centered on the bullet representing the bullet gas and the shock region, respectively. These are immersed in a β -model centered on the main cluster (region j) representing the outer, undisturbed gas. All components are spherically

symmetric around their respective centers; it is an adequate assumption in the sector of interest. Free parameters are the three slopes, two jump amplitudes and two jump radii. A reasonable range of core radii and center positions for the β -model was explored (obviously, these cannot be restricted by the fit) and found to have a small effect on our main interesting parameter, the density jump at the shock. Its confidence interval includes this modeling uncertainty. The observed temperature difference has a negligible effect on the derived density.

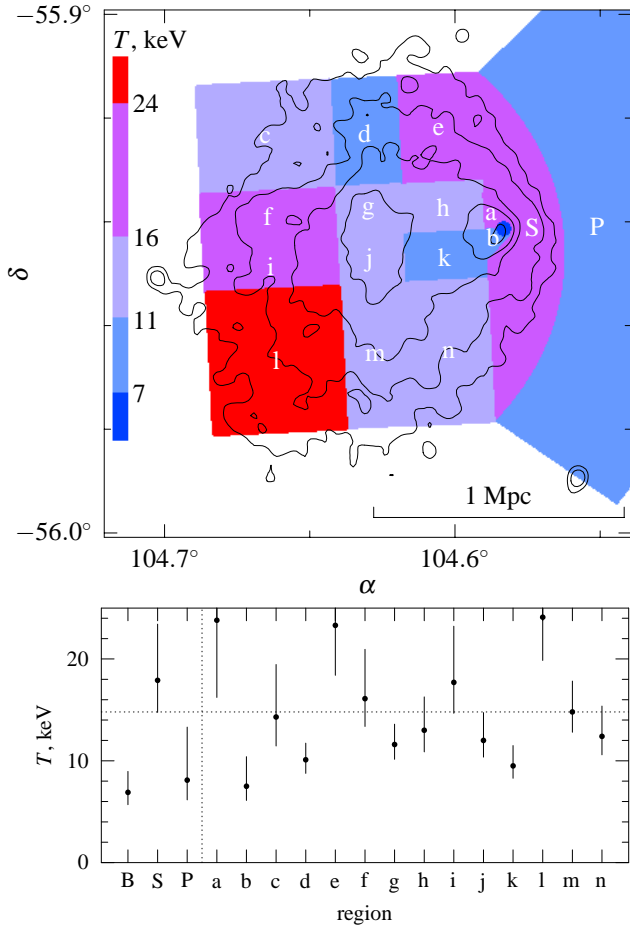


FIG. 2.—Projected gas temperature map (colors) overlaid on the X-ray brightness contours from Fig. 1b. Temperatures for individual regions are shown in lower panel (region *B* is the tip of the bullet, unmarked in the map for clarity. This region appears smaller than the bullet in the contour plot because of smoothing). Errors in this figure are 1σ . The horizontal line shows the cluster average temperature.

The best-fit density model is shown in Fig. 4b; it describes the brightness profile in Fig. 4a well. The best-fit radial slopes are $\alpha \approx 0.15$ for the bullet and $\alpha \approx -0.3$ for the shock region; $\beta \approx 0.7$ assuming a core-radius of $125 h^{-1}$ kpc. The density jumps by factors of $3.8^{+1.3}_{-1.0}$ at the bullet edge and 3.2 ± 0.8 at the shock front. Figure 4b also shows an approximate pressure profile (the density model times the temperatures from Fig. 2). The approximate pressure continuity at the first jump indicates that the bullet boundary is a “cold front”, or contact discontinuity, similar to those recently discovered in other clusters. As expected, there is a large pressure increase at the shock front.

A density jump of 3.2 ± 0.8 at the shock corresponds to a Mach number $M = 3.4$ (> 2.1 at 90%) for a $\gamma = 5/3$ gas and a one-dimensional shock (strictly speaking, the latter approxi-

mation applies only along the direction of the motion, but we can use it as a qualitative estimate for our wide sector). The observed temperature jump from 8^{+9}_{-3} keV to 18^{+9}_{-5} keV corresponds to $M = 2.1 \pm 1.1$ (again, for a qualitative estimate, we assume constant temperatures in regions *P* and *S*). These two independent derivations for the Mach number agree within their 90% uncertainties, and we conclude that $M = 2 - 3$. In the stationary regime, the subcluster should move with the shock velocity. Such Mach numbers and the observed gas temperatures correspond to $v \sim 3000 - 4000$ km s $^{-1}$, implying that the bullet has passed the center of the main cluster ($\sim 0.3 h^{-1}$ Mpc away) just 0.1–0.2 Gyr ago.

In principle, M could also be estimated from the Mach cone: the asymptotic angle φ of the shock w.r.t. the symmetry axis should satisfy $\sin \varphi = M^{-1}$. For $M = 2 - 3$, φ should be $20 - 30^\circ$, whereas the image suggests $\varphi \gtrsim 45^\circ$. A deviation of the velocity vector from the sky plane could widen the Mach cone in projection; however, a sufficiently large inclination angle also would smear the observed sharp brightness edges. An optical measurement of the subcluster relative line of sight velocity in the comoving frame, ~ 800 km s $^{-1}$ (Barrena et al.), combined with our value of M , also indicates only a small ($10 - 15^\circ$) deviation from the sky plane. The Mach cone relation assumes a uniform pre-shock medium and constant velocities, and the cone angle discrepancy is probably due to the cluster’s radially declining density profile and deceleration of the bullet.

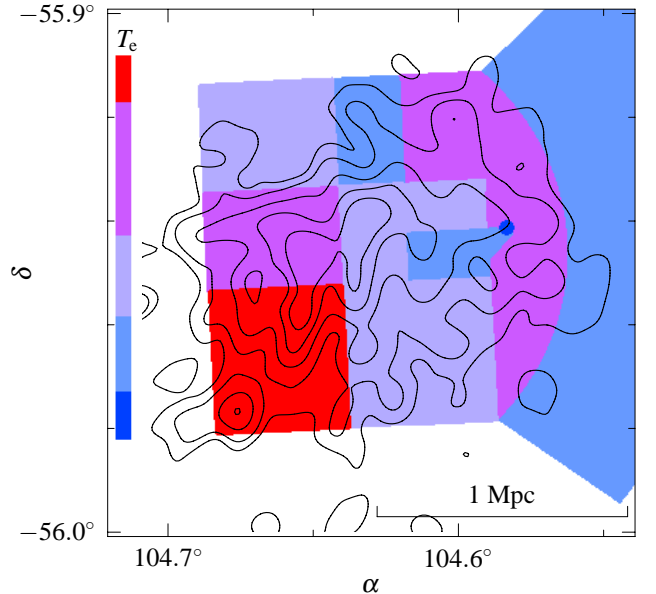


FIG. 3.—Radio halo brightness contours (reproduced from LHBA) overlaid on the temperature map from Fig. 2. The contours are at $(3, 6, 12, 18, 24) \times \sigma$.

4.2. The bullet subcluster

The 0.5–5 keV luminosity of the bullet subcluster is $\sim 5 \times 10^{43} h^{-2}$ erg s $^{-1}$, 10–15% of the typical value for a cluster with the bullet’s temperature; this fraction would change little if adiabatic compression of the bullet by the surrounding hot gas is taken into account. The high gas density in the bullet (Fig. 4b) is of the order of that in the cooling flow clusters at comparable radii. This suggests that the bullet is a remnant of a density peak (cooling flow) that once was at the center of the merging subcluster, perhaps around its brightest galaxy (Fig. 1b). The subcluster’s less dense outer gas was probably shocked and ram

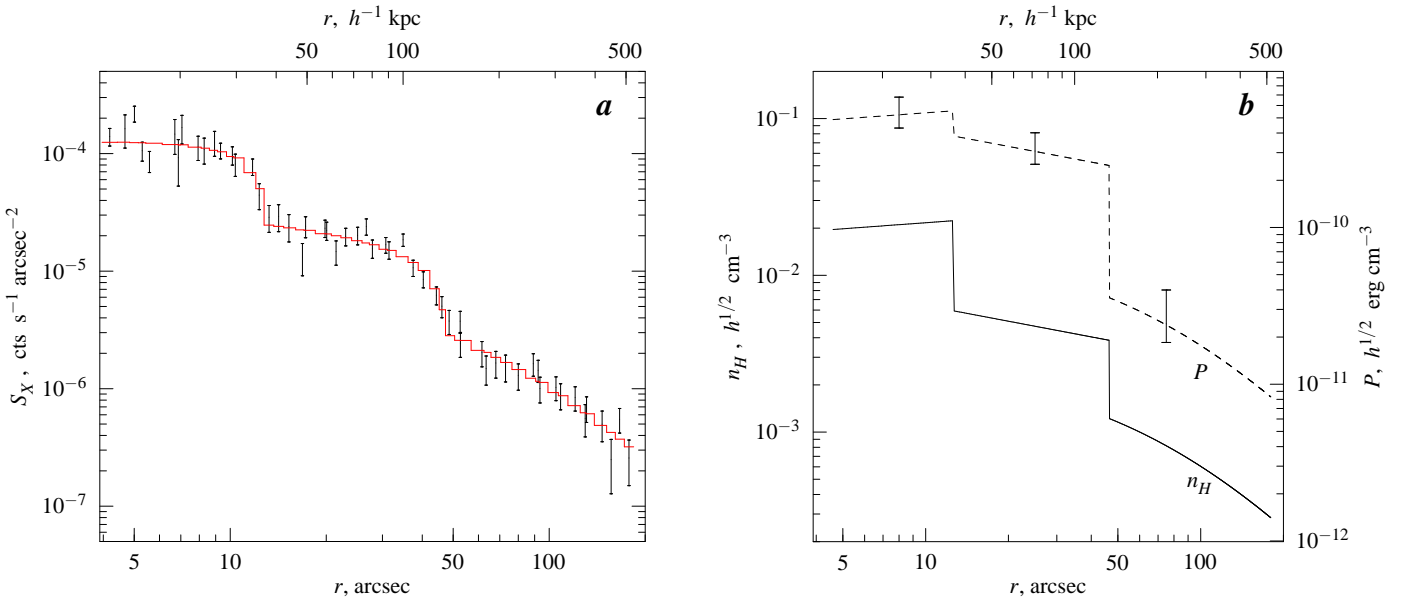


FIG. 4.—(a) ACIS 0.5–5 keV surface brightness profile in a 120° sector centered on the “bullet” and directed westward. The profile is extracted in elliptical segments parallel to the shock front; the r coordinate corresponds to an average radius within a segment. Errors in this figure are 1σ . The histogram shows the best-fit model (see text). The corresponding unprojected model density profile along the symmetry axis is shown in panel (b), which also includes an approximate gas pressure model using temperatures in regions B , S , P from Fig. 2. Error bars on pressure correspond to errors in temperature.

pressure stripped to the radius where the pressures are balanced (see Fig. 4b). Most of the stripped gas may reside in the north-south bar-like structure near the center of the main cluster seen in Fig. 1a (which may be a pancake in projection), since that is where the ram pressure on the moving subcluster was the highest. Disruption of a cooling flow by a merger was considered theoretically by, e.g., Fabian & Daines (1991) and Gómez et al. (2000).

The shuttlecock shape of the bullet clearly shows that it continues to be actively destroyed by gas dynamic instabilities (e.g., Jones, Ryu, & Tregillis 1996). The gas being swept back from the cool bullet appears to be quite hot (region a in Fig. 2) and clumpy (regions a , b), suggesting interesting physics at the interface of the two gases. This interface will be studied in detail using a longer *Chandra* observation planned for 2002.

4.3. High overall temperature

The existence of a few extremely hot clusters such as 1E0657–56 have been used in the past to derive cosmological constraints under the assumption that the high temperature indicates high virial mass. However, the results presented here show that the assumption of hydrostatic equilibrium in 1E0657–56 can easily overestimate the mass by a significant factor due to the ongoing merger and a temporary increase in temperature (see, e.g., simulations by Ricker & Sarazin 2001 and Ritchie & Thomas 2001). It is thus difficult to draw any strong cosmological conclusions without a better estimate of the cluster mass.

4.4. Possible future measurements

The unique shock and supersonic subcluster in 1E0657–56 enable several interesting measurements. Since the gas density and temperature jumps at the shock are related, their accurate measurement may give the equation of state for the intracluster plasma. Magnetic fields, a relativistic particle population with sufficient pressure, a significant lag between the electron and ion temperatures, and large nonthermal energy losses in a

shock could all change the true or the apparent value of γ .

From the velocity of the bullet and the density of the ambient gas, we can derive the ram pressure on the bullet. The gas bullet appears to be pushed away from the subcluster’s dark matter potential well just now, so the gravitational pull of the subcluster should equal the ram pressure. This may give an independent estimate of the subcluster’s total mass (Markevitch et al. 1999).

The cluster also presents an interesting opportunity to constrain the collisional nature of dark matter (e.g., Spergel & Steinhardt 2000; Furlanetto & Loeb 2001). There is a clear offset between the centroid of the bullet subcluster’s galaxies and its gas. If one measures the location of the subcluster’s dark matter density peak (e.g., from weak lensing or detailed modeling of the gas distribution), one may determine whether the dark matter is collisionless, as are the galaxies, or if it experiences an analog of ram pressure, as does the gas.

5. SUMMARY

The *Chandra* observation of 1E0657–56 presents a prototypical example of a merger bow shock. The shock propagates in front of a cooler gas “bullet”, apparently a remnant of a dense central region of the merging subcluster whose outer gas was stripped by ram pressure. The subcluster Mach number is 2–3 and its velocity is 3000 – 4000 km s⁻¹. Thus the subcluster traversed the main cluster core only 0.1–0.2 Gyr ago. The bullet is at the final stage of being destroyed by gas dynamic instabilities. Its gas lags behind the subcluster galaxies due to the ram pressure of the shocked gas. The hottest gas resides in a different region of 1E0657–56 where additional merging activity occurs. The overall high temperature of 1E0657–56 is unlikely to represent its virial temperature due to the ongoing merger.

We thank L. Grego, H. Tananbaum and the referee for useful comments. Support was provided by NASA contract NAS8-39073, grant NAG5-9217, the Smithsonian and the CfA fellowship program.

REFERENCES

Barrena, R., Biviano, A., Ramella, M., Falco, E., & Seitz, S. 2001, Tracing Cosmic Evolution with Galaxy Clusters, eds. S. Borgani et al., ASP Conference Series, in press

Dickey, J. M., & Lockman, F. J. 1990, *ARA&A*, 28, 215

Fabian, A.C., & Daines, S. J. 1991, *MNRAS*, 252, 17P

Furlanetto, S. R., & Loeb, A. 2001, *ApJ*, submitted (astro-ph/0107567)

Furusawa, T., Yamasaki, N., Ohashi, T., Shibata, R., & Ezawa, H. 2001, *ApJL*, in press (astro-ph/0110146)

Gómez, P.L., Loken, C., Roettiger, K., & Burns, J. O. 2000, *ApJ*, in press (astro-ph/0009465)

Govoni, F., Enßlin, T. A., Feretti, L., & Giovannini, G. 2001, *A&A* 369, 441

Jones, T. W., Ryu, D., & Tregillis, I. L. 1996, *ApJ*, 473, 365

Liang, H., Hunstead, R. W., Birkinshaw, M., & Andreani, P. 2000, *ApJ*, 544, 686 (LHBA)

Henry, J. P., & Briel, U. G. 1995, *ApJ*, 443, L9

Kaastra, J. S. 1992, "An X-Ray Spectral Code for Optically Thin Plasmas" (Internal SRON-Leiden Report, updated version 2.0)

Markevitch, M., et al. 2000, *ApJ*, 541, 542

Markevitch, M., Sarazin, C. L., & Vikhlinin, A. 1999, *ApJ*, 521, 526

Markevitch, M., & Vikhlinin, A. 2001, *ApJ*, in press; astro-ph/0105093 (MV)

Neumann, D. M., et al. 2001, *A&A*, 365, L74

Ricker, P. M., & Sarazin, C. L. 2001, *ApJ* in press (astro-ph/0107210)

Ritchie, B. W., & Thomas, P. A. 2001, *MNRAS*, submitted (astro-ph/0107374)

Sarazin, C. L. 2001, Galaxy Clusters and the High Redshift Universe Observed in X-rays, XXXVI Rencontres de Moriond, in press (astro-ph/0105458)

Shafrazev, V. D. 1957, Soviet Phys. JETP, 5, 1183

Spergel, D. N., & Steinhardt, P. J. 2000, *Physical Review Letters*, 84, 3760

Takizawa, M. 1999, *ApJ*, 520, 514

Tribble, P. 1993, *MNRAS*, 263, 31

Tucker, W. H., Tamanbaum, H., & Remillard, R. A. 1995, *ApJ*, 444, 532

Tucker, W., et al. 1998, *ApJ*, 496, L5 (T98)

Vikhlinin, A., Markevitch, M., & Murray, S. S. 2001, *ApJ*, 551, 160

Yaqoob, T. 1999, *ApJ*, 511, L75